Precise probes of type II interferon activity define the origin of interferon signatures in target tissues in rheumatic diseases

John C. Hall[a], Livia Casciola-Rosen[a], Alan E. Berger[b], Efstathia K. Kapsogeorgou[c], Chris Cheadle[b], Athanasios G. Tzioufas[c], Alan N. Baer[a], and Antony Rosen[a,1]

Divisions of [a]Rheumatology and [b]Allergy and Clinical Immunology, Department of Medicine, The Johns Hopkins University School of Medicine, Baltimore, MD 21224; and [c]Laboratory of Immunology, Department of Pathophysiology, School of Medicine, National University of Athens, 11527 Athens, Greece

Edited by Michael B. A. Oldstone, The Scripps Research Institute, La Jolla, CA, and approved September 12, 2012 (received for review June 7, 2012)

Elucidating the molecular pathways active in pathologic tissues has important implications for defining disease subsets, selecting therapy, and monitoring disease activity. The development of therapeutics directed at IFN-α or IFN-γ makes the discovery of probes that report precisely on the activity of different IFN pathways a high priority. We show that, although type I and II IFNs induce the expression of a largely overlapping group of molecules, precise probes of IFN-γ activity can be defined. Used in combination, these probes show prominent IFN-γ effects in Sjögren syndrome (SS) tissues. In contrast, dermatomyositis muscle shows a dominant type I IFN pattern. Interestingly, heterogeneity of IFN signatures exists in patients with SS, with some patients demonstrating a predominant type I pattern. The biochemical patterns largely distinguish the target tissues in patients with SS from those with dermatomyositis and provide a relative weighting of the effects of distinct IFN pathways in specific biopsies. In SS, type I and II IFN effects are localized to the same epithelial cells, surrounded by inflammatory cells expressing IFN-γ–induced proteins, suggesting reinforcing interactions. Precise probes of the different IFN pathways active in tissues of complex rheumatic diseases will be critical to classify disease, elucidate pathogenesis, and select therapy.

autoimmunity | molecular pathology

Defining molecular pathways with precision in pathological tissues has important implications in terms of diagnosis, disease subsetting, monitoring, and therapy. This concept is well illustrated in cancer, where recent studies have demonstrated that very similar clinical and pathological phenotypes encompass multiple molecular subtypes, contributing to different responses to therapy (1–4). It is widely acknowledged that significant heterogeneity exists among patients with autoimmune rheumatic diseases, in terms of phenotype, clinical course, and response to therapy. With the increasing availability of therapies that target specific immune pathways, it has become a priority to define whether the activation of distinct molecular pathways identifies specific subsets of patients within broader phenotypes. The IFN pathways, which have been implicated in the pathogenesis of autoimmune rheumatic diseases, are particularly relevant in this regard.

Sjögren syndrome (SS) is a chronic autoimmune inflammatory disease that targets exocrine glands, particularly salivary and lacrimal glands. Significant evidence implicates IFNs in the pathogenesis of SS including the following: (*i*) increased levels of circulating IFNs in the plasma of SS patients (5); (*ii*) expression of IFN-regulated genes in minor salivary gland biopsies from SS patients (6, 7); (*iii*) the presence of a prominent IFN signature in circulating monocytes and peripheral blood mononuclear cells (PBMCs) from SS patients (8, 9); and (*iv*) the enrichment of plasmacytoid dendritic cells in SS salivary glands (7, 10). Similar IFN signatures have been observed in other rheumatic diseases, including dermatomyositis (DM) (11), polymyositis (12), scleroderma (13), and systemic lupus erythematosus (SLE) (14–16). Interestingly, although several recent papers have suggested that these inflammatory diseases might benefit from inhibition of the type I IFN pathway, studies have shown that inhibition of IFN-α signaling in psoriasis patients (whose skin expresses a prominent IFN signature (17)) had no clinical effect (18). Such data suggest that interpretation of the IFN signature is likely more nuanced than initially conceived, and that additional understanding of the components and mechanisms of the IFN signature is essential. In particular, although the IFN signatures observed in blood and tissues of patients with immune-mediated rheumatic diseases have been attributed to the activity of type I IFNs, contributions of IFN-γ have not been systematically pursued.

In these studies, we initially defined the genes induced by type I and type II IFNs in a human submandibular gland (HSG) epithelial cell line. Unexpectedly, we found that the majority of genes that are highly up-regulated by IFN-α are also highly induced by IFN-γ. In contrast, there was a substantial group of genes that are highly induced by IFN-γ only. To determine whether type I or type II IFN activity was present in minor salivary gland biopsies from patients with SS, we selected and validated precise probes that report on the distinct IFN pathways. Protein expression in minor salivary gland biopsies from SS patients and controls was evaluated by immunoblotting and immunohistochemistry. IFN-regulated proteins were expressed at high levels in SS patients in a pattern consistent with the activity of both type I and type II IFN. However, there was heterogeneity between patients, with evidence of type I IFN-preferential or IFN-γ–preferential patterns. The dominant pattern in SS was quite distinct from that seen in DM, where a more prominent type I IFN pattern was evident. In SS, the cellular distribution of probes of different IFN pathways was also noteworthy: IFN-γ–specific probes were localized to salivary epithelial cells and inflammatory cells in adjacent regions, whereas IFN-α–preferential markers were expressed mostly in salivary epithelial cells in regions that also demonstrate IFN-γ activity.

Together, these data demonstrate that most components of the classically defined type I IFN signature are also well induced by type II IFN, making the signature a broad marker of IFN activity, and not exclusively of type I IFN. Quantification of the specific markers of type II IFN activity is essential to define the origin of

Author contributions: J.C.H., L.C.-R., and A.R. designed research; J.C.H., L.C.-R., and A.E.B. performed research; A.G.T. and A.N.B. contributed new reagents/analytic tools; J.C.H., L.C.-R., A.E.B., E.K.K., C.C., and A.R. analyzed data; and J.C.H., L.C.-R., A.E.B., E.K.K., C.C., A.G.T., A.N.B., and A.R. wrote the paper.

The authors declare no conflict of interest.

This article is a PNAS Direct Submission.

Freely available online through the PNAS open access option.

Data deposition: The microarray data reported in this paper have been deposited in the Gene Expression Omnibus (GEO) database, www.ncbi.nlm.nih.gov/geo. (accession no. GSE41291).

[1]To whom correspondence should be addressed. E-mail: arosen@jhmi.edu.

This article contains supporting information online at www.pnas.org/lookup/suppl/doi:10.1073/pnas.1209724109/-/DCSupplemental.

the IFN-induced protein expression pattern seen in cells and tissues. In target tissues, these probes allow different IFN patterns to be discerned, enabling more precise molecular classification of patient subpopulations. With the availability of new therapeutics targeting type I and type II IFNs, such probes may prove useful for selecting and monitoring therapy, and for defining efficacy of novel agents in the autoimmune rheumatic diseases.

Results

Genes Most Strongly Induced by IFN-α Are also Induced by IFN-γ. To define the origin of the IFN signature in minor salivary gland biopsies from patients with SS, microarray studies were initially performed in an HSG cell line to define IFN-α and IFN-γ responses in a disease-relevant cell type. We selected concentrations of IFN-α and IFN-γ that induced equivalent levels of Ro52 expression (IFN-α, 1,000 U/mL; IFN-γ, 50 ng/mL) (Fig. S1). We set Ro52 as our reference molecule, because it is a frequent autoantigen in SS and is known to be induced by both IFN-α and IFN-γ. Because protein expression in target tissues provides an integrated view of events that have occurred over time before biopsy, we analyzed IFN-induced gene expression at 4, 12, 24, and 48 h. We identified 416 mRNA transcripts that were significantly induced [fold change, ≥2.0; value of $P \leq 0.01$; false discovery rate (FDR), ≤0.25] by IFN-α or IFN-γ at one or more time points (lists of transcripts are provided in Tables S1, S2, S3, and S4). We first compared the induction of all 416 transcripts by IFN-α and IFN-γ at each time point and made several important observations (Fig. 1 *A–D*). (*i*) The largest number of IFN-α–induced transcripts ($n = 165$) was seen at 12 h (Fig. 1*B*). In contrast, the IFN-γ response lagged significantly, with the maximal number of IFN-γ–induced transcripts ($n = 285$) detected at 48 h (Fig. 1*D*). (*ii*) There were few transcripts exclusively induced by IFN-α at any time point (Fig. 1 *A–D*, red triangles); except for a single transcript at 4 h (Fig. 1*A*), all IFN-α–specific transcripts were induced eightfold (i.e., a $\log_2$ fold change of 3) or less. Notably, however, >50% of IFN-γ–responsive transcripts were induced exclusively by IFN-γ (Fig. 1 *C* and *D*, blue squares). Of these, 10 were induced eightfold or greater at 24 h and 23 were induced eightfold or greater at 48 h. (*iii*) The majority of transcripts induced highly by IFN-α were also induced by IFN-γ (Fig. 1 *A–D*, green circles). Additionally, the levels of induction by IFN-α were significantly higher in the IFN-α/γ–responsive group than the IFN-α–specific group (at 24 h, $P = 0.01$; Wilcoxon rank sum test) (Fig. 1*C*). Similarly, the levels of induction by IFN-γ were higher in the IFN-α/γ–responsive group than the IFN-γ–specific group (at 24 h, $P = 5.4 \times 10^{-12}$; Wilcoxon rank sum test).

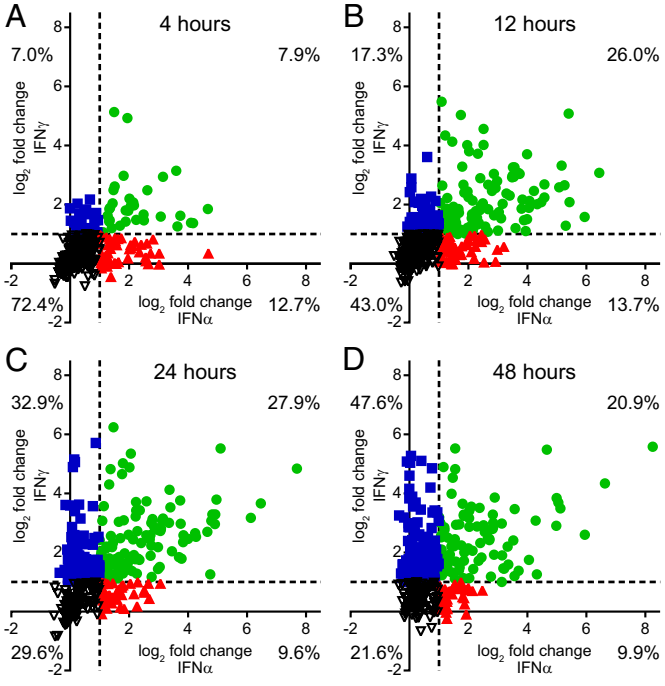

Fig. 1. Temporal analysis of IFN-α and IFN-γ responses in HSGs. Expression of the 416 IFN-inducible transcripts at (*A*) 4, (*B*) 12, (*C*) 24, and (*D*) 48 h. Data are presented as $\log_2$ fold change in expression relative to untreated cells. The transcripts in each group are represented as follows: IFN-γ specific (blue squares), IFN-α/γ responsive (green circles), IFN-α specific (red triangles), and uninduced (open triangles). The percentage of transcripts in each group is listed. The dashed lines indicate a twofold increase in expression.

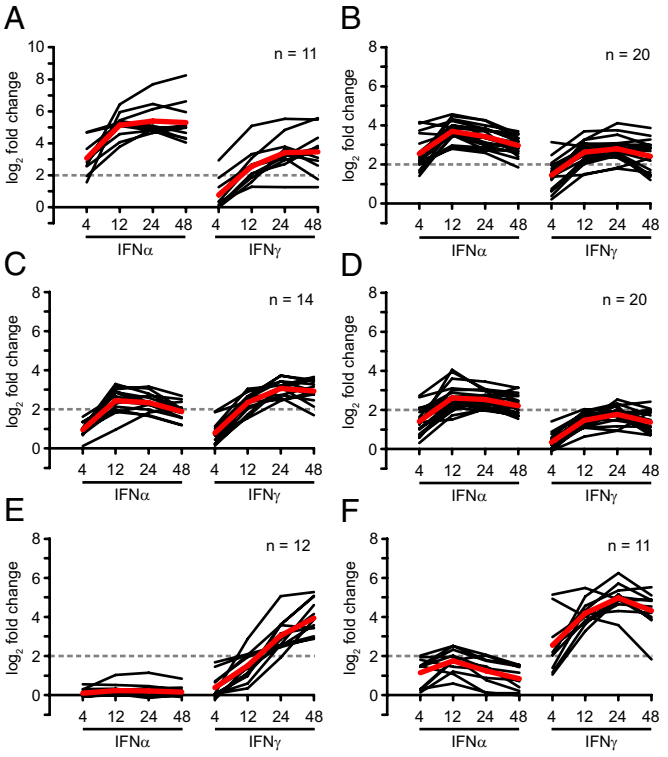

Fig. 2. Analysis of IFN-inducible gene expression using SOMs. The 416 IFN-inducible transcripts were clustered into 16 groups. The mean induction values were calculated for each group of transcripts at each time point (4, 12, 24, or 48 h) and the groups with the highest mean expression in response to IFN-α (*A–D*) and IFN-γ (*A*, *E*, and *F*) are shown (the remaining maps are presented in Figs. S2 and S3). Individual transcripts are shown in black. Mean values for the group at each time point are shown in red. The *y*-axis represents $\log_2$ fold change in expression relative to untreated cells. The dashed lines indicate a fourfold increase in expression.

To identify groups of probes that distinguish between the activity of IFN-α and IFN-γ across all time points, gene expression data were subjected to unsupervised clustering using self-organizing maps (SOMs). The 416 IFN-induced transcripts were clustered into 16 groups, and the mean level of induction in response to IFN-α and IFN-γ at each time point was calculated for each group. We compared mean induction across all groups, and several major findings were evident. First, there are few transcripts that are specific reporters of an IFN-α response. Of the four groups of transcripts ($n = 65$) (Fig. 2 *A–D*) that exhibited the highest mean induction in response to IFN-α, three groups ($n = 45$) (Fig. 2 *A–C*) were induced on average fourfold or greater by IFN-γ at two or more time points. Interestingly, many of the genes associated with the IFN signature defined in DM and SLE were among these transcripts (Table S5), highlighting that these signatures are not

necessarily IFN-α specific. In contrast, two of the three groups of transcripts ($n = 34$) with the highest mean induction by IFN-γ (Fig. 2 *A*, *E*, and *F*) were either exquisitely specific (Fig. 2*E*; $n = 12$) or highly preferential (Fig. 2*F*; $n = 11$) for IFN-γ activity. An additional four groups ($n = 87$) of transcripts exhibited either low differential expression, which occurred at only one time point, or were IFN-γ specific only at 48 h (Fig. S2). The remaining six groups, which included the majority of IFN-responsive transcripts ($n = 241$; 57.9%), were induced, on average, less than fourfold by IFN-α and IFN-γ across all time points (Fig. S3). Thus, these probes have limited utility as markers of an IFN response. These data demonstrate that detecting genes highly induced by IFN-α cannot distinguish clearly between the activity of IFN-α and IFN-γ, particularly if the timing of the stimulus is unknown. In contrast, quantifying markers uniquely and highly induced by IFN-γ provides a potentially useful set of probes to distinguish the origin of an IFN signature observed in vivo.

Biochemical Validation of Probes of IFN Activity. We next sought to confirm these patterns at the level of protein expression. We treated HSGs with IFN-α or IFN-γ for 4, 12, 24, or 48 h and immunoblotted equivalent amounts of protein lysates. We tested antibodies recognizing several IFN-α and IFN-γ–preferential genes to select the highest quality probes for use in differentiating between IFN-α and IFN-γ activity in human tissues (Fig. 3). Several observations were relevant: (*i*) IFN-inducible proteins were not detectable in untreated cells; (*ii*) as defined in the optimization phase, Ro52 was induced to equivalent levels by IFN-α and IFN-γ at 24 and 48 h; (*iii*) the IFN-α response was rapid, with maximal expression of MDA5, IFIT3, and Ro52 detected at 12 h; this remained elevated through 48 h; (*iv*) the IFN-γ response occurred more slowly, with protein expression peaking at 48 h; (*v*) MDA5 and IFIT3 were IFN-α specific at 12 h but were IFN-γ responsive (albeit at markedly lower levels than the IFN-α response) at 24 and 48 h; (*vi*) GBP1 and GBP2 were robustly and specifically induced by IFN-γ only; (*vii*) a low dose of IFN-γ enhanced the expression of MDA5 and IFIT3 in IFN-α–treated cells, whereas IFN-α did not enhance the induction of GBP1 and GBP2 (Fig. S4). Quantifying the expression of IFN-γ–specific proteins (e.g., GBP1, GBP2) in human tissues is therefore necessary to accurately differentiate between IFN-α and IFN-γ activity in vivo.

Type I and Type II IFN Activity Is Prominent in Minor Salivary Gland Biopsies from SS Patients. To define the IFN pathways represented in SS, we analyzed protein expression in lysates of minor salivary

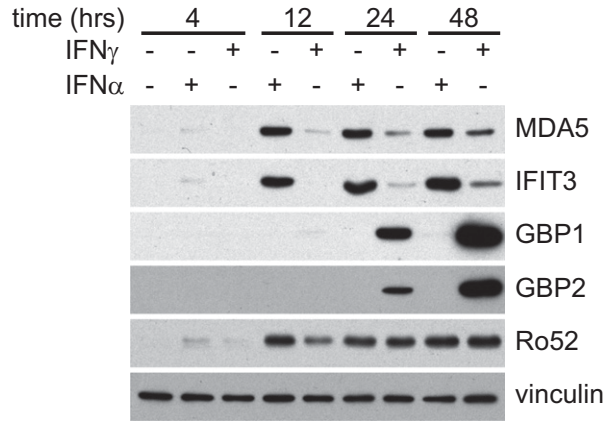

Fig. 3. Validating probes of IFN-α and IFN-γ activity. Equivalent amounts of protein lysates from HSGs cultured for 4, 12, 24, or 48 h in the absence or presence of IFN-α (1,000 U/mL) or IFN-γ (50 ng/mL) were analyzed by Western blotting. Antibodies against IFN-α–specific, IFN-γ–specific, and IFN-α/γ–responsive molecules as defined by array were used. Vinculin is included as a loading control.

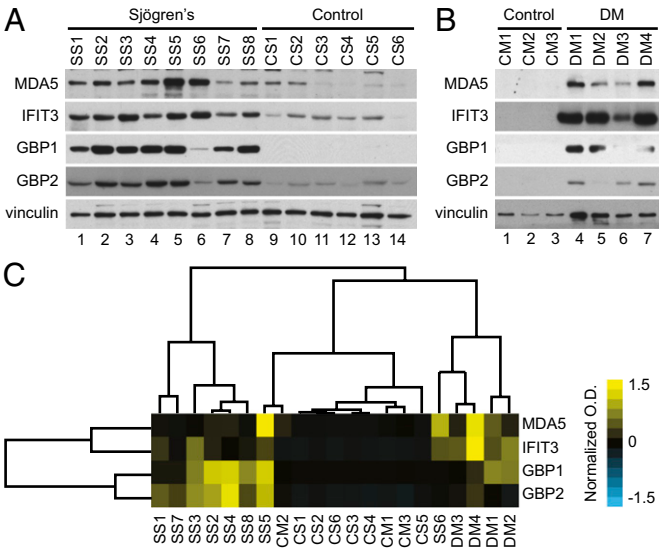

Fig. 4. Distinct patterns of type I and type II IFN-induced proteins in SS and DM tissue biopsies. (*A*) Protein lysates made from control (CS, $n = 6$) and SS (SS, $n = 8$) MSG biopsies were probed for IFN-inducible protein expression by Western blotting. Markers of type I IFN (MDA5, IFIT3) and type II IFN (GBP1, GBP2) were analyzed. Vinculin is included as a loading control. (*B*) Protein lysates made from control (CM, $n = 3$) and DM (DM, $n = 4$) muscle biopsies were probed with markers of type I and type II IFN. Vinculin is included as a loading control. (*C*) IFN-induced protein expression from *A* and *B* was quantified by densitometry and normalized to the level of vinculin expression in the respective sample. Vinculin-normalized expression values were median centered and subject to unsupervised hierarchical clustering to define patterns of IFN-induced protein expression in individual patients.

gland biopsies from SS patients ($n = 8$) and controls ($n = 6$). These samples were immunoblotted with antibodies against IFIT3, MDA5, GBP1, GBP2, and vinculin (loading control). Although IFN-induced protein expression was generally low or absent in control salivary glands, some heterogeneity was noted, particularly for MDA5 and IFIT3, which likely reflects variability in baseline expression levels. In SS, striking increases in the expression of MDA5, IFIT3, GBP1, and GBP2 were evident in most patients, indicating both type I and type II IFN effects in most biopsies (Fig. 4*A*). Although six of eight patients had elevated expression of both IFN-α– and IFN-γ–induced proteins, there was some variation in patterns between individual patients, with one patient exhibiting a predominantly IFN-α pattern (Fig. 4*A*, lane 6) and one demonstrating a predominantly IFN-γ pattern (Fig. 4*A*, lane 7).

To define whether markers of both type I and type II IFNs were similarly present in tissues from another autoimmune rheumatic disease in which an IFN signature is prominent, we analyzed muscle tissue from patients with DM. Expression of the panel of IFN-induced molecules was examined in control ($n = 3$) and DM ($n = 4$) muscle biopsy lysates by immunoblotting (Fig. 4*B*). IFN-inducible proteins were not detected in control muscle. In contrast to SS tissues, there was marked expression of IFIT3 in DM muscle with comparably lower expression of GBP1 and GBP2, suggestive of a type I IFN response in these samples. To compare the patterns in SS and DM, the data were quantified by densitometry and the expression levels of IFIT3, MDA5, GBP1, and GBP2 were normalized to the expression level of a loading control, vinculin, in each sample. The normalized data were subjected to unsupervised hierarchical clustering to define subgroups (Fig. 4*C*). Interestingly, the IFN-α–preferential markers and the IFN-γ–specific markers clustered separately. With a single exception (SS6), SS patients were clearly separated from controls and from DM patients. SS6

had a predominant type I IFN pattern, and was more similar to DM than either SS or controls.

Evidence of both Type I and II IFN Activity in Salivary Gland Epithelial Cells. We next defined the cells in SS salivary glands that express markers of type I and type II IFN effects by immunohistochemistry. Serial sections of four SS and three control salivary glands were stained, and representative data from two SS patients are shown in Fig. 5. Minimal IFIT3 and GBP2 staining was seen in control salivary glands (Fig. 5 *A* and *D*). Expression of IFIT3 and GBP2 was increased in SS salivary gland biopsies, consistent with the biochemical studies. The predominant staining pattern showed IFIT3 expression mainly in salivary duct epithelial cells, particularly in regions surrounded by inflammatory cells (Fig. 5 *B* and *C*). Minimal IFIT3 staining was observed in infiltrating inflammatory cells. In contrast, GBP2 was prominently expressed in the nuclei of infiltrating inflammatory cells. GBP2 staining was also evident in salivary ducts, where the nuclei of both infiltrating inflammatory cells (strong staining) as well as duct epithelium were stained (moderate staining). Interestingly, GBP2 and IFIT3 stained the same regions of the ducts that were surrounded by GBP2-positive inflammatory cells (Fig. 5 *E* and *F*). Isotype control antibody staining was negative for all samples (Fig. S5).

Discussion

The autoimmune rheumatic diseases are a complex group of disorders that display considerable heterogeneity in phenotype, immune response, disease course, and response to therapy. Defining whether distinct molecular subgroups exist may facilitate novel disease classification and allow more precise selection of therapy. The IFN pathways are particularly relevant in this regard.

The finding of an IFN signature in the blood and tissue of many autoimmune inflammatory diseases (11–16) has important potential for disease monitoring and therapy. Although there is significant evidence implicating type I IFNs in the generation of the IFN signature in SLE, it remains unclear whether type I IFNs are the primary driver of the IFN signature in other rheumatic processes. Indeed, previous microarray studies have shown that, although IFN-induced proteins are differentially expressed in SS salivary glands relative to controls (6), the activities of IFN-α and IFN-γ could not be distinguished (7). The enrichment of activated lymphocytes (robust sources of IFN-γ secretion) in inflamed tissues in the rheumatic diseases (19, 20) reinforces the possible contributions of IFN-γ to the IFN signature observed in tissues. The failure of a recent trial of an anti–IFN-α monoclonal antibody in psoriasis (which expresses a strong IFN signature) (18), coupled with the finding that expression of IFN signatures is prominent in many different inflammatory diseases, underscores the need to improve our understanding of the origins and meaning of the IFN signature in different inflammatory diseases in vivo.

Previous studies analyzing IFN-induced gene expression in various cell types in vitro have been limited in their ability to interpret signatures observed in tissues, because they frequently only address a single time point and use arbitrary doses of IFN. Diseased tissues encompass events that have occurred asynchronously before tissue sampling. We therefore performed extensive gene expression analysis to determine the kinetics of the responses and identify probes that differentiate between type I and type II IFN effects at multiple time points. Because autoantigen expression in target tissues is likely a critical partner in driving the autoimmune response (21, 22), we selected doses of IFN-α and IFN-γ that induced equivalent amounts of Ro52, an IFN-induced autoantigen frequently targeted in SS. The extensive similarity of the patterns of gene expression in response to type I and type II IFNs was quite remarkable. Of the gene products induced twofold or more by IFN-α, 38% (at 4 h) to 74% (at 24 h) were also induced twofold or more by IFN-γ. Interestingly, the IFN signatures defined to date in rheumatic disease samples largely include these IFN-α/γ–induced genes. These signatures cannot discriminate between the effects of type I and type II IFNs. We defined a cassette of molecules whose expression is strongly induced by, and highly specific for, type II IFN activity (e.g., GBP1, GBP2) across all time points after IFN exposure. Given the high degree of specificity of the defined probes for IFN-γ effects, these markers should be included in analyses of IFN responses in tissues, to either confirm, or rule out, IFN-γ activity. These data also highlight the importance of recognizing the cellular and kinetic heterogeneity of tissues when interpreting gene expression patterns in health and disease. Definition of specific markers of pathways, which maintain their specificity across a range of times, is both feasible and useful.

We used these tools to quantify the origins of IFN signatures in normal and diseased human tissues. Because multiple pathways may be activated simultaneously in diseased tissue, we used a simple combination of IFN-α–preferential probes with IFN-γ–specific probes to quantify the activity of the different IFN pathways. Heterogeneity in IFN pathway activation was observed in different SS salivary glands. In most patients, evidence of both

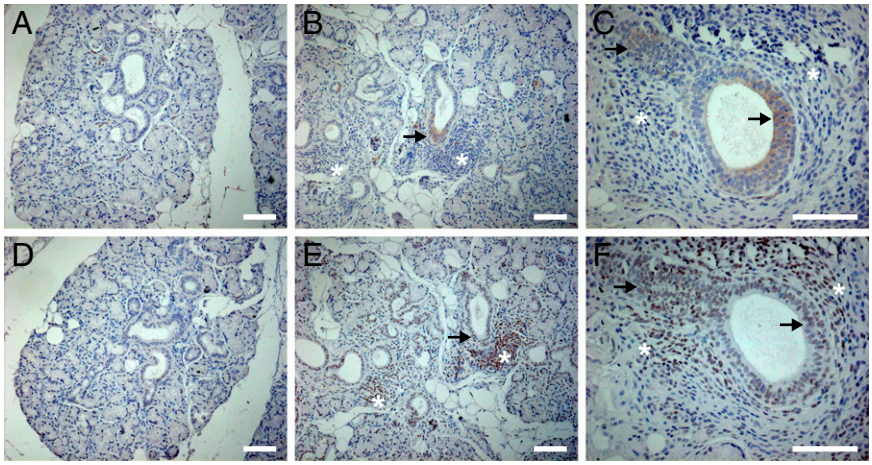

Fig. 5. Colocalization of markers of type I and type II IFN activity in SS salivary gland biopsies. Minor salivary gland biopsies from controls ($n = 3$) and patients with SS ($n = 4$) were stained with antibodies against the type I IFN-preferential protein IFIT3 (*A*–*C*) and the IFN-γ–specific protein GBP2 (*D*–*F*). Representative images from one control (*A* and *D*) and two SS (*B*, *C*, *E*, and *F*) biopsies are shown. Staining with isotype control antibodies was negative in all samples (shown in Fig. S5). The asterisks denote areas of inflammation, and the arrows designate salivary gland epithelial cells that express both IFIT3 and GBP2. (Scale bars, 50 μm.)

type I and II IFN activity was present. In some patients, there was evidence of either predominant type I (patient SS6) or type II IFN activity (patient SS7). This was in contrast to a small cohort of DM patients who exhibited predominantly IFN-α activity. The four probes chosen in our initial analysis could identify relevant subgroups when protein expression in biopsies was quantified by densitometry, normalized against a loading control, and subjected to unsupervised hierarchical clustering. Diseased tissues were clearly separated from control tissues. Quite strikingly, SS tissues were separated from DM tissues, except for the single SS outlier that exhibited a predominantly type I IFN pattern, which clustered with DM patients. It is noteworthy that just four IFN-induced proteins were sufficient to distinguish these groups. The analysis is simple and quantitative, requires very small amounts of tissue, provides an integrated readout of pathways active in the target tissues, and has the potential for automation. This approach facilitates a more precise classification of patients based on activity of specific pathways in the target tissue. It has significant potential as a molecular diagnostic to more precisely delineate disease subsets, and assist in selecting patients for therapy or for monitoring effectiveness.

Although the presence of IFN signatures in the target tissue in rheumatic diseases has been well defined, there has not been an opportunity to simultaneously visualize the activity of IFN-α and IFN-γ by immunohistochemistry in the same tissues. Our studies demonstrate some interesting findings in this regard. First, expression of IFIT3 and GBP2 was enriched in the same areas of SS salivary glands. Second, IFIT3 and GBP2 were both expressed in salivary epithelial cells located in areas of significant inflammatory infiltrate, although the patterns differed. IFIT3 staining was enriched in ductal epithelial cells and did not stain inflammatory cells with similar intensity. In contrast, although GBP2 expression in ductal epithelial cells in inflamed areas was clearly evident, expression of GBP2 was more prominent in surrounding infiltrating mononuclear cells. These patterns demonstrate that epithelial cells in areas of inflammation in the SS glands are showing the effects of both types of IFNs. This localized distribution suggests that the type I and type II IFN pathways converge in epithelial cells at these sites. Because small amounts of type II IFN can enhance IFIT3 expression (Fig. S4) induced by type I IFN, it is possible that the striking IFIT3 staining in SS epithelium reflects the sensitizing effects of local IFN-γ. It is also possible that the ability of IFN-γ to enhance signaling through Toll-like receptors (TLRs) (e.g., TLR3), with augmentation of type I IFN secretion and downstream pathways (23), may enhance the type I IFN effect in the presence of relevant TLR ligands. It is noteworthy that some of the prominent ribonucleoprotein autoantigens targeted in autoimmune rheumatic diseases like SS can ligate and activate TLRs (10, 24, 25). The existence of positively reinforcing interactions between the different IFN pathways in SS may provide important therapeutic opportunities. Quantifying IFIT3 and GBP2 expression in the target tissue during therapy with inhibitors of specific IFN pathways may provide important insights into the nature and direction of these reinforcing interactions.

The finding of an IFN-γ effect in SS tissues is noteworthy given that IFN-γ has many potential roles in the pathogenesis of SS. IFN-γ can induce MHC and costimulatory molecule expression on epithelial cells, potentially enabling their function as antigen-presenting cells in the disease microenvironment (26). IFN-γ has also been shown to sensitize cells to death-inducing stimuli (27). IFN-γ induces the expression of BAFF (28), which may play a role in dysregulating B-cell responses in SS. Last, IFN-γ has been shown to decrease SERCA pump activity and Ca^{2+} stores in HSGs (29, 30) and alter tight junction structure and function in rat parotid cell line (31), possibly contributing to the functional defects in secretion in SS exocrine tissue. Understanding whether IFN-γ plays a role in driving pathology in SS is an important priority.

Although an IFN signature has been defined in the blood of patients with SS and other autoimmune conditions (where it is associated with active disease), it is not yet known whether the blood signature has the same pattern as that in affected tissue in the different diseases. Our studies do not address this important issue because of the lack of availability of PBMCs from patients with frozen biopsies. However, a recent study observed high levels of expression of genes that we show to be IFN-γ specific at multiple time points (e.g., GBP1, WARS, and SERPING1) in PBMCs from SS patients (9), suggesting that an IFN-γ effect is present in peripheral blood. It is possible that lymphocytes that infiltrate the target tissue in SS enter the tissue with the IFN-γ effect established and play an upstream role in mediating functional effects in the target tissue. Defining with precision the origin of the IFN signature in circulating cells in different diseases is an important priority. The data will provide tools to quantify responses to therapeutic measures, and potentially the kinetics of movement of these cells into and out of tissues during therapy.

These studies have defined probes that more precisely quantify the activity of different IFN pathways in tissues from various inflammatory rheumatic diseases. Using such probes on human tissue has demonstrated that different rheumatic phenotypes associated with an IFN signature have distinct patterns of IFN activity, which are not evident using other analyses. Furthermore, heterogeneity in signatures exists even within a disease phenotype, suggesting the probes defined here may be useful markers of patient subsets, where specific IFNs play distinct roles. As new therapeutic agents that inhibit type I or type II IFNs become available, it will be essential to identify with precision the activity of that pathway in vivo at baseline and after therapy. The approach and tools defined here provide potentially powerful ways to accomplish this.

Materials and Methods

Cell Culture and IFN Treatment. Cells from an HSG epithelial cell line (32), a gift from Bruce Baum (National Institutes of Health/National Institute of Dental and Craniofacial Research, Bethesda, MD), were maintained in MEM supplemented with 10% (vol/vol) FBS and 2 mM L-glutamine. Cells were cultured as noted in the presence of purified leukocyte IFN-α (Sigma) or IFN-γ (R&D Systems).

Microarray Analysis. HSGs were cultured for 4, 12, 24, or 48 h either with IFN-α (1,000 U/mL) or IFN-γ (50 ng/mL), or without IFN added, and samples were collected in triplicate at each time point; 36 total samples were assayed. Total RNA was extracted using TRIzol (Invitrogen). Additional purification was performed on RNeasy columns (Qiagen), and total RNA quality was assessed using an Agilent 2100 Bioanalyzer (Agilent Technologies). Biotin-labeled cRNA was prepared from total RNA according to the chip manufacturer's protocol (Illumina). cRNA was hybridized to Illumina Human HT12 v3 Expression BeadChips, and signal was detected with streptavidin-Cy3. Signal intensity quantification was performed using an Illumina BeadStation 500GX Genetic Analysis Systems scanner. The microarray data discussed in this publication have been deposited in the National Center for Biotechnology Information's Gene Expression Omnibus (33).

Analytical Methods and Statistical Analysis for Microarray Data. A single intensity (expression) value for each Illumina probe was obtained using Illumina BeadStudio software with standard settings and no background correction. The expression values for all of the probes for each sample were scaled to have median of 256 (2^8) and then $\log_2$ transformed. Gene expression in IFN-α– and IFN-γ–treated cells was compared against untreated cells at each time point. Transcripts (i.e., Illumina probes) considered to be differentially expressed between two groups of samples were those satisfying the following criteria: (*i*) Welch *t* test values of $P \leq 0.01$ (34); (*ii*) Benjamini-Hochberg FDR of ≤0.25 (35); (*iii*) a fold change of >2.0 (calculated using geometric means); and (*iv*) the expression value of the transcript is above the Illumina BeadStudio calculated background (detection *P* value of <0.01) in all three samples in the group with the higher average expression level for that probe, thus avoiding false positives based on background noise and also reducing the number of statistical tests for the subsequent FDR calculation. For a given probe, if the average of the expression levels in the control samples is greater than that for the IFN-treated samples, then the ratio of the control average to the IFN average is given, with a minus sign in front, so the fold change magnitude is always at least 1. SOM analysis was performed

in GenePattern 2.0 (36) using the SOM clustering algorithm with final α and σ values of 0.005 and 0.5, respectively (37).

Patients and Tissues. Minor salivary gland (MSG) biopsies were obtained with informed consent from individuals undergoing diagnostic evaluation for sicca symptoms indicative of SS, under the approval of the Ethical Committee of School of Medicine of the National University of Athens (Athens, Greece; Protocol 5107). SS patients were diagnosed on the basis of the revised American–European classification criteria (38). The control group included individuals complaining of sicca symptoms, who did not fulfill the aforementioned SS criteria and had negative biopsy focus scores (<1 foci/4 mm^2). None of the individuals studied had evidence of lymphoma, sarcoidosis, or infection by hepatitis B, hepatitis C, or HIV. Frozen minor salivary gland biopsies (for lysate generation) were obtained from eight SS patients and six controls. Salivary gland paraffin sections were obtained from four SS patients and three controls.

Muscle biopsies were obtained from patients seen at the Neuromuscular Clinic at Johns Hopkins Hospital. Informed consent was obtained from every study subject, and all samples were collected under the auspices of Johns Hopkins Medicine Institutional Review Board-approved protocols. All patient samples were deidentified, with clinical and laboratory features linked only to the patient code. Surgical procedures were performed for patient management, and the research tissue samples were excess tissue obtained for routine diagnostic purposes. Frozen muscle biopsies were obtained from four patients with DM and three individuals whose biopsies were histologically normal. Histologic criteria for biopsies identified as DM were consistent with Bohan and Peter criteria (39, 40).

Determination of Antigen Expression in Cultured Cells and Human Tissues. Lysates were prepared on ice as described previously (21). Protein equivalents were electrophoresed on SDS-polyacrylamide gels, transferred onto nitrocellulose membranes, and probed with antibodies recognizing GBP1, Ro52 (Santa Cruz Biotechnology), IFIT3, vinculin (Sigma-Aldrich), GBP2 (Novus Biologicals), or MDA5 (American Research Products). Visualization was performed using horseradish peroxidase-conjugated secondary antibodies (Jackson Immunoresearch) and developed using an enhanced chemiluminescence detection system (Pierce). For densitometry, X-ray films were scanned using an AGFA Arcus II scanner, and densities were quantified using Bio-Rad Quantity One software. Hierarchical clustering of protein expression was performed in GenePattern 2.0 using the Hierarchical Clustering algorithm (41) and was visualized using Java TreeView (42).

Immunohistochemistry. Salivary gland paraffin sections were processed as described previously (43). Briefly, after rehydration, antigen retrieval, and blocking, sections were incubated overnight at 4 °C with either anti-IFIT3 (10 μg/mL; Novus) or GBP2 antibodies (30 μg/mL; Novus Biologicals). HRP-conjugated secondary antibody incubations were performed for 1 h at room temperature, and staining was visualized with diaminobenzidine (Dako) per the manufacturer's directions. Nuclei were counterstained with Mayer's hematoxylin. Negative controls were performed using isotype control antibodies, and in all cases no staining was detected. All images were captured using a Zeiss Axioskop 50 with a Zeiss AxioCam HRc camera and AxioVision 4 software.

ACKNOWLEDGMENTS. This work was supported by National Institutes of Health Grants DE 12354, DE 12354-12S1, AR 053503, and AR 44684; The Dorothy L. and Donald S. Stabler Foundation; and The Jerome L. Greene Foundation.

1. Druker BJ, et al. (2001) Efficacy and safety of a specific inhibitor of the BCR-ABL tyrosine kinase in chronic myeloid leukemia. *N Engl J Med* 344(14):1031–1037.
2. Radich JP, et al. (2006) Gene expression changes associated with progression and response in chronic myeloid leukemia. *Proc Natl Acad Sci USA* 103(8):2794–2799.
3. Corless CL, Heinrich MC (2008) Molecular pathobiology of gastrointestinal stromal sarcomas. *Annu Rev Pathol* 3:557–586.
4. Bertos NR, Park M (2011) Breast cancer—one term, many entities? *J Clin Invest* 121 (10):3789–3796.
5. Hooks JJ, et al. (1979) Immune interferon in the circulation of patients with autoimmune disease. *N Engl J Med* 301(1):5–8.
6. Hjelmervik TO, Petersen K, Jonassen I, Jonsson R, Bolstad AI (2005) Gene expression profiling of minor salivary glands clearly distinguishes primary Sjögren's syndrome patients from healthy control subjects. *Arthritis Rheum* 52(5):1534–1544.
7. Gottenberg JE, et al. (2006) Activation of IFN pathways and plasmacytoid dendritic cell recruitment in target organs of primary Sjögren's syndrome. *Proc Natl Acad Sci USA* 103(8):2770–2775.
8. Wildenberg ME, van Helden-Meeuwsen CG, van de Merwe JP, Drexhage HA, Versnel MA (2008) Systemic increase in type I interferon activity in Sjögren's syndrome: A putative role for plasmacytoid dendritic cells. *Eur J Immunol* 38(7):2024–2033.
9. Emamian ES, et al. (2009) Peripheral blood gene expression profiling in Sjögren's syndrome. *Genes Immun* 10(4):285–296.
10. Båve U, et al. (2005) Activation of the type I interferon system in primary Sjögren's syndrome: A possible etiopathogenic mechanism. *Arthritis Rheum* 52(4):1185–1195.
11. Greenberg SA, et al. (2005) Interferon-alpha/beta-mediated innate immune mechanisms in dermatomyositis. *Ann Neurol* 57(5):664–678.
12. Walsh RJ, et al. (2007) Type I interferon-inducible gene expression in blood is present and reflects disease activity in dermatomyositis and polymyositis. *Arthritis Rheum* 56 (11):3784–3792.
13. Tan FK, et al. (2006) Signatures of differentially regulated interferon gene expression and vasculotrophism in the peripheral blood cells of systemic sclerosis patients. *Rheumatology (Oxford)* 45(6):694–702.
14. Baechler EC, et al. (2003) Interferon-inducible gene expression signature in peripheral blood cells of patients with severe lupus. *Proc Natl Acad Sci USA* 100(5):2610–2615.
15. Bennett L, et al. (2003) Interferon and granulopoiesis signatures in systemic lupus erythematosus blood. *J Exp Med* 197(6):711–723.
16. Han GM, et al. (2003) Analysis of gene expression profiles in human systemic lupus erythematosus using oligonucleotide microarray. *Genes Immun* 4(3):177–186.
17. Yao Y, et al. (2008) Type I interferon: Potential therapeutic target for psoriasis? *PLoS One* 3(7):e2737.
18. Bissonnette R, et al. (2010) A randomized, double-blind, placebo-controlled, phase I study of MEDI-545, an anti-interferon-alfa monoclonal antibody, in subjects with chronic psoriasis. *J Am Acad Dermatol* 62(3):427–436.
19. Grassi M, Capello F, Bertolino L, Seia Z, Pippione M (2009) Identification of granzyme B-expressing CD-8-positive T cells in lymphocytic inflammatory infiltrate in cutaneous lupus erythematosus and in dermatomyositis. *Clin Exp Dermatol* 34(8):910–914.
20. Christodoulou MI, Kapsogeorgou EK, Moutsopoulos HM (2010) Characteristics of the minor salivary gland infiltrates in Sjögren's syndrome. *J Autoimmun* 34(4):400–407.
21. Casciola-Rosen L, et al. (2005) Enhanced autoantigen expression in regenerating muscle cells in idiopathic inflammatory myopathy. *J Exp Med* 201(4):591–601.
22. Mammen AL, et al. (2009) Expression of the dermatomyositis autoantigen Mi-2 in regenerating muscle. *Arthritis Rheum* 60(12):3784–3793.
23. Negishi H, et al. (2008) A critical link between Toll-like receptor 3 and type II interferon signaling pathways in antiviral innate immunity. *Proc Natl Acad Sci USA* 105 (51):20446–20451.
24. Båve U, Alm GV, Rönnblom L (2000) The combination of apoptotic U937 cells and lupus IgG is a potent IFN-alpha inducer. *J Immunol* 165(6):3519–3526.
25. Lau CM, et al. (2005) RNA-associated autoantigens activate B cells by combined B cell antigen receptor/Toll-like receptor 7 engagement. *J Exp Med* 202(9):1171–1177.
26. Tsunawaki S, et al. (2002) Possible function of salivary gland epithelial cells as nonprofessional antigen-presenting cells in the development of Sjögren's syndrome. *J Rheumatol* 29(9):1884–1896.
27. Kulkarni K, Selesniemi K, Brown TL (2006) Interferon-gamma sensitizes the human salivary gland cell line, HSG, to tumor necrosis factor-alpha induced activation of dual apoptotic pathways. *Apoptosis* 11(12):2205–2215.
28. Ittah M, et al. (2006) B cell-activating factor of the tumor necrosis factor family (BAFF) is expressed under stimulation by interferon in salivary gland epithelial cells in primary Sjögren's syndrome. *Arthritis Res Ther* 8(2):R51.
29. Wu AJ, et al. (1996) Interferon-gamma induced cell death in a cultured human salivary gland cell line. *J Cell Physiol* 167(2):297–304.
30. Meehan S, Wu AJ, Kang EC, Sakai T, Ambudkar IS (1997) Interferon-gamma induces a decrease in the intracellular calcium pump in a human salivary gland cell line. *Am J Physiol* 273(6 Pt 1):C2030–C2036.
31. Baker OJ, et al. (2008) Proinflammatory cytokines tumor necrosis factor-alpha and interferon-gamma alter tight junction structure and function in the rat parotid gland Par-C10 cell line. *Am J Physiol Cell Physiol* 295(5):C1191–C1201.
32. Wu AJ, et al. (1994) Effect of tumor necrosis factor-alpha and interferon-gamma on the growth of a human salivary gland cell line. *J Cell Physiol* 161(2):217–226.
33. Edgar R, Domrachev M, Lash AE (2002) Gene Expression Omnibus: NCBI gene expression and hybridization array data repository. *Nucleic Acids Res* 30(1):207–210.
34. Pan W (2002) A comparative review of statistical methods for discovering differentially expressed genes in replicated microarray experiments. *Bioinformatics* 18(4):546–554.
35. Benjamini Y, Hochberg Y (1995) Controlling the false discovery rate: A practical and powerful approach to multiple testing. *J R Stat Soc B* 57:289–300.
36. Reich M, et al. (2006) GenePattern 2.0. *Nat Genet* 38(5):500–501.
37. Tamayo P, et al. (1999) Interpreting patterns of gene expression with self-organizing maps: Methods and application to hematopoietic differentiation. *Proc Natl Acad Sci USA* 96(6):2907–2912.
38. Vitali C, et al. (2002) Classification criteria for Sjögren's syndrome: A revised version of the European criteria proposed by the American-European Consensus Group. *Ann Rheum Dis* 61(6):554–558.
39. Bohan A, Peter JB (1975) Polymyositis and dermatomyositis (first of two parts). *N Engl J Med* 292(7):344–347.
40. Bohan A, Peter JB (1975) Polymyositis and dermatomyositis (second of two parts). *N Engl J Med* 292(8):403–407.
41. de Hoon MJ, Imoto S, Nolan J, Miyano S (2004) Open source clustering software. *Bioinformatics* 20(9):1453–1454.
42. Eisen MB, Spellman PT, Brown PO, Botstein D (1998) Cluster analysis and display of genome-wide expression patterns. *Proc Natl Acad Sci USA* 95(25):14863–14868.
43. Levine SM, et al. (2007) Novel conformation of histidyl-transfer RNA synthetase in the lung: The target tissue in Jo-1 autoantibody-associated myositis. *Arthritis Rheum* 56 (8):2729–2739.